Probing Single-Molecule T4 Lysozyme Conformational Dynamics by Intramolecular Fluorescence Energy Transfer

Yu Chen, Dehong Hu, Erich R. Vorpagel, and H. Peter Lu*

Fundamental Science Division, Pacific Northwest National Laboratory, P.O. Box 999, Richland, Washington 99352

Received: November 12, 2002; In Final Form: March 3, 2003

We demonstrate the use of single-molecule spectroscopy to study enzyme conformational motions of T4 lysozyme under hydrolysis reaction of the polysaccharide walls of *E. coli* B cells. By attaching a donor−acceptor pair of dye molecules site-specifically to noninterfering sites on the enzyme, the hinge-bending motions of the enzyme are measured by monitoring the donor−acceptor emission intensity as a function of time. The overall enzymatic reaction rate constants are found to vary widely from molecule to molecule. The dominant contribution to this static inhomogeneity is attributed to enzyme searching for reactive sites on the substrate. We have also applied molecular dynamics simulation and a random-walk model to analyze the enzyme−substrate complex formation dynamics, revealing multiple intermediate conformational states in the chemical reaction process. This approach provides information about the microscopic conformational change drifting velocity, diffusion coefficient, friction coefficient, energy consumed by friction along the reaction coordinate, and energy landscape.

Although enzymatic reactions are traditionally studied at the ensemble level, the inhomogeneities of the reaction dynamics, the correlated enzyme conformational motions, and the nonsynchronizable nature of these complex reactions make it extremely difficult to obtain stepwise mechanistic and dynamic information from such studies. Single-molecule enzymatic reactions have been studied under physiological conditions in recent years.[1−14] Single-molecule assays have revealed static[2,3,6,9,10] and dynamic[6,9,10] disorder in the dynamics of single-molecule enzymatic reactions,[1−3] coenzyme redox state turnovers in real time,[6] and enzymatic reaction product formation in real time.[9,10] Static disorder and dynamic disorder[15−19] are, respectively, the static rate inhomogeneities between molecules and the dynamic rate fluctuations for individual molecules. Dynamic disorder, which is not distinguishable from static disorder in an ensemble-averaged measurement, has been attributed to protein conformational fluctuations.[6,9,10] Presumably, the protein conformational motions at the active site of the enzyme are most critically responsible for the inhomogeneities in the enzymatic reactions.[6,9,10] Although real-time probing of the associate conformational changes for motor proteins under enzymatic reactions has been reported,[12] direct observation of conformational changes along the enzymatic reaction coordinate for many other reaction systems, including T4 lysozyme enzymatic hydrolysis reaction systems, is still a highly challenging task. We report real-time single-molecule measurements of the T4 lysozyme protein hinge-bending motion during the course of sequential enzymatic reaction turnovers. The resulting single-molecule reaction trajectories and their statistical analyses provide new insights into the mechanism and dynamics of the T4 lysozyme enzymatic reaction.

The wild-type T4 lysozyme has two domains connected by an α-helix.[20−23] It catalyzes the hydrolysis of polysaccharide chains of an *E. coli* B cell-wall matrix. The structure and enzymatic activity of wild-type T4 lysozyme and its mutants have been investigated extensively by X-ray crystallography,[20−23] NMR,[24−28] and EPR.[29] The proteins have been shown to adopt different conformations, which can be described as two domains undergoing a hinge-bending motion.[20−25,29,30] There are different degrees of opening of the active site due to the hinge-bending motion for various mutants of T4 lysozyme, which have been measured by NMR and crystallography in the absence of a substrate. The crystal structure of a T4 lysozyme−substrate complex, where the substrate molecule is covalently linked to the active site of the enzyme,[23] shows no significant domain displacement comparing the enzyme−substrate complex and the enzyme. This will be shown later to be consistent with our findings that, after the enzyme has opened and bound to the substrate, it returns to its initial overall geometry to form the bound complex in an activated state. Although EPR study suggested 8 Å hinge-bending closing upon substrate binding,[29] there have been no direct observations of how much the active site opens to initiate the formation of an enzyme−substrate complex under physiological conditions. In an enzymatic reaction, the protein domain motions in general under a substrate-free condition can be dramatically different compared to the protein domain motion under the substrate interaction. The difficulties for ensemble-averaged and static structure measurements are that the dynamic enzyme−substrate intermediate states are extremely difficult to measure, if not impossible. Our knowledge of the dynamic domain hinge-bending motions of the T4 lysozyme has not been able to be obtained from direct structure measurements so far. The results of our and others'[30] molecular dynamics simulations and single-pair fluorescence resonant energy transfer (spFRET) trajectories suggest that the relative domain displacement between open and closed states can be as large as 4.5 Å. Our molecular dynamics (MD) simulation results show that the Arg 137−Glu 22 salt bridge between domains at the doorway of the enzyme active

* To whom correspondence should be addressed. E-mail: peter.lu@pnl.gov.

10.1021/jp022406z CCC: $25.00
Published on Web 07/16/2003

site plays a critical role in the transition of the open and closed conformational states of the enzyme.

Although the hydrolysis reaction mechanism of T4 lysozyme has been extensively studied and the structure of the T4 lysozyme reaction intermediate has been reported,[23] there are difficulties in characterizing the dynamics of T4 lysozyme due to the complexity of the substrate. The current enzymatic reaction assay uses light-scattering from the cell wall[31] and the release of lipoprotein[32] from the cell wall to measure the reaction progress. These measured parameters can give only a rough estimate of the reaction rate. In this work, we explore a new approach of single-molecule spectroscopy to study the complex enzymatic reaction and characterize the dynamics of T4 lysozyme by the corresponding conformational change at the single-molecule level. Previous single-molecule enzymatic reaction studies have used either a fluorescence product[9,10] or a fluorescent enzyme[6] to probe the reaction. These approaches have the advantage of direct measurements of the enzymatic reaction turnovers and product, but the reaction-related specific conformational changes of the enzyme are difficult to study using these approaches. Because it is still extremely hard to probe simultaneous single-molecule turnovers, product generation, and specific conformational changes by a single-molecule spectroscopic measurement, there is typically a tradeoff in probing one parameter that is most critical for a molecular-level understanding of the mechanism of a particular enzymatic reaction system. However, enzymatic reactions often involve a complex environment and mechanism; therefore, it is often crucial to probe directly the specific conformational changes involved in an enzymatic reaction. The hinge-bending motions associated with the T4 lysozyme hydrolysis enzymatic reaction are critical but cannot be studied by either conventional ensemble-averaged measurements or the above-mentioned single-molecule spectroscopic approaches. In this paper, we report work using intramolecular fluorescence resonance energy transfer[7,8,33,34] between a single pair of dye molecules labeling T4 lysozyme to probe the conformational change during enzymatic reaction. Our approach has the advantage of characterizing the enzymatic-activity-related conformational fluctuation, although the product release is not directly probed.

Materials and Methods

Site-Specific Donor−Acceptor Dye Labeling. T4 lysozyme and mutants were provided by Prof. Brian Matthews at the University of Oregon. We labeled the protein by thiolation to Cys 54 and Cys 97 following the standard protocol from Molecular Probes, Inc. Site specificity was achieved by exploiting the reactivity difference of maleimide and iodoacetamide with the partially buried and spatially restricted Cys 54. We used Texas Red maleimide and tetramethylrhodamine (TMR) iodoacetamide from Molecular Probes to label wild-type T4 lysozyme consecutively. We purified the product after each labeling step by gel filtration and hydrophobic interaction chromatography; 70% of the final product was single TMR- and single Texas Red-labeled protein verified by MALDI-TOF measurements. Figure 1A shows the ensemble-averaged emission spectrum of TMR- and Texas Red-labeled T4 lysozyme excited at 530 nm, which is used for all single-molecule studies in this work. The donor−acceptor fluorescence intensity ratio at 570 nm/600 nm is 0.8 and independent of either the excitation wavelength from 500 to 532 nm or labeled protein concentration over a 4-fold change. The donor−acceptor absorption (Figure 1A, inset) and emission (Figure 1A) spectra ratios also provide evidence of intramolecular FRET. The significant advantage of our site-specific covalent dye labeling is that the attached donor−acceptor pair can sense the relative motion of the two domains in T4 lysozyme without perturbation of the enzymatic activity. As expected for dye substitution at locations that are far from the active site (Figure 1), the activity of the labeled wild-type protein is identical with that of an unlabeled wild-type protein verified by enzymatic reaction assay.[35]

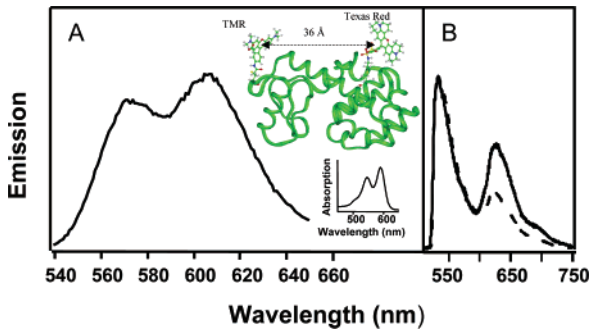

Figure 1. Ensemble-averaged spectroscopy control results. (A) Fluorescence spectra of tetramethylrhodamine- and Texas Red-labeled 240 nM T4 lysozyme excited at 530 nm. The absorption spectrum is plotted in the inset. The crystal structure of wild-type T4 lysozyme with two dye molecules is shown in the inset as well. (B) Fluorescence spectra of Alexa 488/Alexa 594-labeled T4 lysozyme mutant (E11A) excited at 488 nm. The solid and dashed lines are the fluorescence spectra of the enzyme in solution without and with substrate *E. coli* B cell walls present, respectively. The two spectra are normalized to the same maximum point to aid the view.

To confirm that spFRET provides the sensitive measurement of the conformational change of T4 lysozyme under enzymatic reactions, we have also labeled a T4 lysozyme mutant (E11A) with a single donor−acceptor pair of Alexa 488 and Alexa 594 maleimides for the purpose of an ensemble-averaged control experiment. Because in the mutant E11A the two cysteine groups are equally accessible to thiolation reaction, two dyes were used to label the two cysteine groups nonselectively. We did not separate the mixture of donor−donor-, donor−acceptor-, and acceptor−acceptor-labeled E11A. Nevertheless, only the donor−donor- and donor−acceptor-labeled proteins are optically excitable, and they can be differentiated by their distinctively different emission spectra. High water solubility of the Alexa dyes leads to a higher yield of protein labeling, which is desirable for an ensemble-averaged control experiment needing a larger quantity of samples.

Single-Molecule and Ensemble-Averaged T4 Lysozyme Hydrolysis Assays. The substrate of T4 lysozyme is peptidoglycan from the *E. coli* B cell wall. Peptidoglycan, a major component of the bacterial cell wall, is a cross-linked polymer containing polysaccharide and amino acids. It is prepared from lyophilized *E. coli* B cell (Sigma), according to a previously used lipid-removing procedure.[31] The peptidoglycan product is a PBS buffer suspension of 1-μm particles of cell-wall fragments. It is typically further broken down to submicrometer size by sonication. The cell walls are considered porous, although we have not characterized the surface morphology. No oxygen scavenger agents were used in our experiments.

The ensemble-averaged enzyme activity is presented by the decrease of light-scattering from the substrate at unit time. However, this commonly used assay is not a quantitative assay due to the complexity of the substrate. This hydrolysis reaction often has an "incubation time" when the T4 lysozyme enzymatic reactive interactions with the substrate occur at a slow rate or less efficiently due to the relatively lower density of the binding sites at the substrate. Under such a reactive enzyme−substrate interaction, the "incubation process" involves an increased

surface area, change in fragment morphology, and removal of surface protection layer, etc., before a normal reaction occurs. The dye-labeled T4 lysozyme remains the same activity as the unlabeled one. However, we have not tested the activity of surface-tethered T4 lysozyme because the peptidoglycan assay is not sensitive enough for the limited number of enzyme molecules on the surface. In the single-molecule reaction, we introduce nanomolar unlabeled T4 lysozyme into the substrate solution for the purpose of "incubation" to maintain the normal reaction condition of the surface-tethered dye-labeled T4 lysozyme enzyme. The precise turnover time of the enzymatic reaction is still unknown in the literature. We estimated the number of bonds cleaved per second on the basis of the weight of the cell wall digested per second at a certain enzyme concentration. Our single-molecule data are an attempt to experimentally measure the turnover time.

Single-Molecule and Ensemble-Averaged FRET. Studies of single-molecule T4 lysozyme conformational dynamics during an enzymatic reaction are made possible by applying the technique of spFRET.[7,8,33,34] Besides our current study, a previous[30] molecular dynamics simulation of wild-type T4 lysozyme in solution showed that a distance change of the two cysteine groups between the closed and open states occurs; we have calculated that the distance change between the two dye-tethered cysteine residues is from 30.5 to 35 Å; i.e., the donor−acceptor distance change is about 4.5 Å. Considering the lengths of the two covalent linking groups of the donor and acceptor dipoles, the actual donor−acceptor dipole−dipole distance change is estimated to be ∼5.5 Å. We estimated the Förster distance R_0[6] of both a TMR/Texas Red pair and the Alexa 488/Alexa 594 pair to be about 50 ± 5 Å. The donor fluorescence intensity, I_D, is calculated by I_0, the donor fluorescence intensity without the acceptor, and R, the distance between the donor and acceptor: $I_D = I_0/[1 + (R_0/R)^6]$.

At this R_0, the distance change of 5.5 Å, from around 30 to around 35 Å, can cause a change in donor fluorescence intensity by a factor of 2−3, although the change of the acceptor fluorescence intensity is less than 10%. Hence, it is feasible to probe the 5.5 Å donor−acceptor distance change by monitoring the change of the I_D.

The domain motion of T4 lysozyme is rather complex and contains motions besides hinge-bending. For example, the domain rotational motion along the α-helix has been predicted by MD simulation.[36] The domain rotational motion can also contribute to the spFRET efficiency change because the rotational motion involves both the dipole orientation change and the dipole−dipole distance change of the two dyes. However, there is no definitive experimental evidence supporting the existence of this type of rotational motion involved in the enzymatic reaction. It is reasonable to assume that the hinge-bending motion in nature involves multiple coupled nuclear coordinates that can be projected to a nuclear coordinate associated with the α-helix. Although the MD simulation in this paper is not used to determine the FRET efficiency quantitatively, it nonetheless helps in understanding which enzymatic reaction step induces an increase or decrease in FRET efficiency.

To demonstrate the feasibility of applying FRET to probe the conformational changes of T4 lysozyme proteins under binding and unbinding hinge-bending motions, we measured the ensemble-averaged FRET emission spectra from the donor−acceptor-labeled T4 lysozyme, both with and without a substrate. Although the wild type is the best candidate for such a measurement, the enzymatic reaction is too fast even for the concentration of the dye-labeled enzyme at the detection limit of a fluorometer, and the substrate concentration cannot be maintained at a constant level within seconds of the spectrum-collection time. Consequently, we used the mutant E11A instead, which has binding and unbinding activity but does not catalyze the hydrolysis of the substrate. Figure 1B shows the emission spectra of the donor−acceptor-labeled proteins in a buffer solution without (solid line) and with (dashed line) the addition of substrate *E. coli* B cell walls. The ratio of spectral intensities of the donor emission vs acceptor emission increases with attachment to the substrate. Modeling the expected motions during opening of the enzyme active-site region shows that the donor−acceptor distance will increase, decreasing the efficiency of donor−acceptor energy transfer and yielding the observed increase in the donor−acceptor spectral intensity ratio.

The contribution to the donor−acceptor spectral intensity change of the ensemble-averaged measurement has to include additional factors besides FRET. The apparent donor−acceptor intensity ratio change in this ensemble-averaged measurement may not be equal to the ratio change in the single-molecule FRET measurement. The T4 lysozyme mutant E11A sample contains donor−donor-labeled product, for which the distance change is associated with the self-quenching effect.[37,38] The distance increase between the two donors reduces the self-quenching and consequently increases the donor fluorescence intensity. The fraction of time of an "open" state during the enzymatic reaction also has an important influence on the donor−acceptor intensity ratio change. This donor−donor self-quenching effect enhances the measured donor−acceptor emission intensity ratio difference with and without the substrate (Figure 1B). Nevertheless, the ensemble fluorescence intensity measurement indicates the conformation change of T4 lysozyme upon binding to the substrate, although it is essentially a qualitative confirmation of FRET existence under the interaction between the enzyme and substrate.

Experimental Setup. The T4 lysozyme was covalently linked to a silanized glass coverslip by the bifunctional linker SIAXX (Molecular Probes, Inc.). A confocal microscope with 532 nm CW excitation (1−10 μW) from a diode-pumped solid-state laser was used to image the individual protein molecules and measure the single-molecule fluorescence intensity trajectories.[39] The excitation was circularly polarized to minimize the intensity fluctuation due to rotation of the proteins. The donor and acceptor fluorescence signals were split by a dichroic beam splitter and imaged onto a pair of photon-counting avalanche photodiodes with appropriate optical filters[6,8,40] for recording the separate emission intensities. The donor TMR and acceptor Texas Red emissions were detected separately by a pair of avalanche photodiode detectors after passing through a 570 nm band-pass filter (20 nm bandwidth) and a 615 nm long-pass filter, respectively. The acceptor has a negligible contribution at a wavelength of 570 ± 10 nm compared to the donor emission. However, above a 615 nm wavelength, an approximately 15% leakage of donor fluorescence to the acceptor channel cannot be avoided due to the emission spectral overlap. The "cross-talking" also exists in 532 nm excitation. The acceptor Texas Red can be weakly excited by the excitation laser, which cannot be avoided. However, cross-talking in detection only contaminates the acceptor signal but not the donor signal. It does not cause the intensity fluctuation of either the donor or acceptor emission channel. On the other hand, for the Alexa 488 and Alexa 594 pair, both the emission peaks and absorption peaks are well separated and cross-talking is negligible.

Molecular Dynamics Simulation. MD calculations were carried out using the NWChem software package[41] and the all-atom Amber99 (param99)[42] force field or Discover with the default CVFF force field. NWChem molecular dynamics simulations were carried out under periodic boundary conditions in the constant-pressure, constant-temperature ensemble at 300 K and 1 atm, with weak (τ = 0.1 ps) Berendsen temperature and pressure coupling and SHAKE to constrain hydrogen bonds and allow a 2.0 fs time step. The particle-mesh Ewald method was used for electrostatic interactions with a grid spacing of about 1.1 Å. Chloride ions were added to produce a net neutral charge. Lennard-Jones interactions were evaluated using a 9.0 Å atom-based cutoff. For Discover simulations, a distance-dependent dielectric was used ($1/4r^2$) with a cutoff of 15.0 Å with only crystallographic water molecules included. To keep the water from "evaporating", a small (default) force was applied to tether the oxygen atoms to their original positions.

Results and Discussion

Single-Molecule Spectroscopic Control Experiments. Figure 2A shows dual fluorescence intensity trajectories simultaneously recorded from a donor−acceptor-labeled T4 lysozyme in the presence of substrate at pH 7.2. The anticorrelated fluctuations (Figure 2A,B) are due to spFRET, reporting the donor−acceptor distance change associated with the protein conformational motion. Anticorrelated features in donor−acceptor fluorescence intensity were not observed in the absence of a substrate (Figure 2C,D). Therefore, we attribute this conformational motion to an enzyme-related motion, most likely the open−closed hinge-bending motion of the T4 lysozyme under enzymatic reaction conditions. This attribution is consistent with the results of the ensemble-averaged FRET measurements made with and without substrate (Figure 1B). Further evidence that we are measuring the hinge-bending motion comes from evaluating autocorrelation functions calculated from the single-molecule trajectories when the laser excitation intensity and the physiological conditions of pH and substrate concentration are changed.

Each single-molecule trajectory (Figure 2A) is analyzed by calculating the autocorrelation function, in which the decay rate constant is the sum of the forward and backward rate constants on the basis of a two-state model[43] (assuming that there are essentially two conformational states involved in the enzymatic reaction). Although the enzymatic reaction involves more than two states in this system, the autocorrelation function decay rate proportionally reflects the overall reaction rate. The observed autocorrelation decay rate constants are related to the enzymatic reaction rate constants. It should be carefully noted that the quantitative evaluation of the autocorrelation rate constants relies on the nature of the fluctuation. For a special type of fluctuation, two-state switching kinetics, "on−off" blinking of the single molecule, the average times that the molecule stays in the "on" state and "off" state are τ_{on} and τ_{off}, respectively. The autocorrelation rate ($1/\tau_c$) is the sum of the two transition rates ($1/\tau_c = 1/\tau_{on} + 1/\tau_{off}$), and the overall reaction rate is $1/\tau = (1/(\tau_{on} + \tau_{off}))$.[6,17,44] So, the autocorrelation rate ($1/\tau_c$) is at least 4 times larger than the reaction rate ($1/\tau$). In general, if the two types of fluctuation are under different nuclear coordinates, the autocorrelation function shows biexponential decay with two rate constants. On the other hand, if the two types of fluctuation are under the same nuclear coordinate, the autocorrelation rate constant is the sum of the two fluctuation rate constants. For a T4 lysozyme enzymatic reaction, the fluctuation rate can be further increased by intensity fluctuations due to intrastate conformational changes that are at a higher rate than that of the enzymatic reaction. These intrastate conformational fluctuations are associated with the nuclear coordinates that are coupled

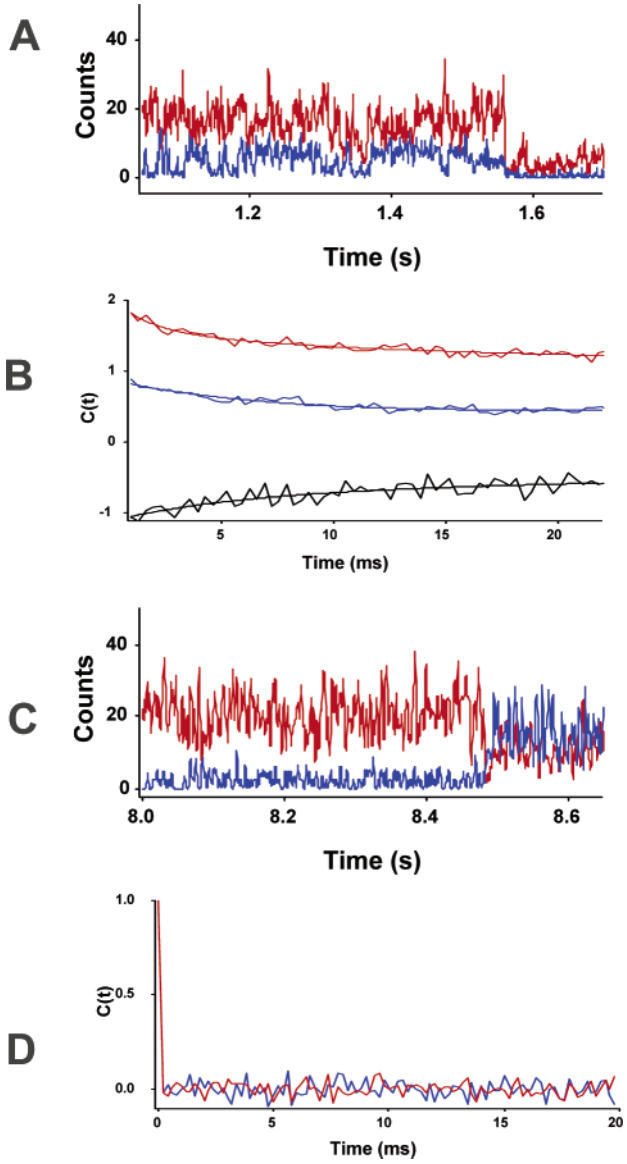

Figure 2. Single-molecule recording of T4 lysozyme conformational motions and enzymatic reaction turnovers of hydrolysis of an *E. coli* B cell wall in real time. (A) shows a pair of trajectories from a fluorescence donor tetramethylrhodamine (blue) and acceptor Texas Red (red) pair in a single T4 lysozyme in the presence of *E. coli* cells of 2.5 mg/mL in pH 7.2 buffer. Anticorrelated fluctuation features are evident. (B) Correlation functions ($C(t)$) of the donor ($\langle \Delta I_d(0) \Delta I_d(t) \rangle$, blue) and acceptor ($\langle \Delta I_a(0) \Delta I_a(t) \rangle$, red) (autocorrelation) and donor−acceptor ($\langle \Delta I_d(0) \Delta I_a(t) \rangle$, black) (cross-correlation) deduced from the single-molecule trajectories in (A). They are fitted with the same decay rate constant of 180 ± 40 s^{-1}. A long decay component of 10 ± 2 s^{-1} is also evident in each autocorrelation function. The first data point (not shown) of each correlation function contains the contribution from the measurement noise and fluctuations faster than the time resolution. The correlation functions are normalized, and $\langle \Delta I_a(0) \Delta I_a(t) \rangle$ is presented with a shift on the y axis to enhance the view. (C) A pair of fluorescence trajectories from a donor (blue) and acceptor (red) pair in a T4 lysozyme protein without substrates present. The acceptor was photobleached at about 8.5 s. (D) Correlation functions ($C(t)$) of the donor ($\langle \Delta I_d(0) \Delta I_d(t) \rangle$, blue) and acceptor ($\langle \Delta I_a(0) \Delta I_a(t) \rangle$, red) derived from the trajectories in (C). The autocorrelation function only shows a spike at $t = 0$ and drops to zero at $t > 0$, which indicates that only uncorrelated measurement noise and fluctuation faster than the time resolution were recorded.

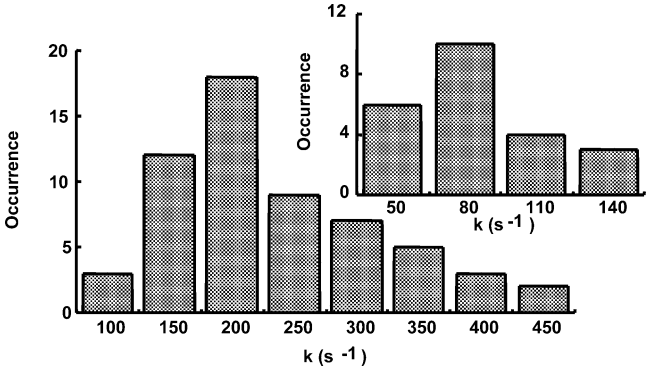

Figure 3. Distribution of donor autocorrelation decay rate constants (k) derived from 59 single-molecule trajectories measured at pH 7.2. The inset shows the distribution of autocorrelation decay rate constants (k) derived from 23 single-molecule trajectories measured at pH 6.0. Although the lengths of the trajectories are different due to photobleaching, the autocorrelation time has no bias from trajectory length because the autocorrelation time is much shorter than the photobleaching time.

to the hinge-bending nuclear motions. The fluorescence intensity trajectories of the donor ($I_d(t)$) and acceptor ($I_a(t)$) give autocorrelation times (Figure 2B) indistinguishable from fitting an exponential decay to the autocorrelation functions $\langle \Delta I_d(0)\ \Delta I_d(t)\rangle$ and $\langle \Delta I_a(0)\ \Delta I_a(t)\rangle$, where $\Delta I_d(t)$ is $I_d(t) - \langle I_d\rangle$, $\langle I_d\rangle$ is the mean intensity of the overall trajectory of a donor, and $\Delta I_a(t)$ has the same definition for an intensity trajectory of an acceptor. In contrast, the cross-correlation function between the donor and acceptor trajectories, $\langle \Delta I_d(0)\ \Delta I_a(t)\rangle$, is anticorrelated with the same decay time (Figure 2B), which supports our assignment of anticorrelated fluctuations of the fluorescence intensities of the donor and acceptor to the spFRET process. We varied the laser excitation power to yield a detected fluorescence counting rate ranging from 2.5×10^3 to 1×10^5 counts/s and calculated the fluctuation correlation times of the single-molecule trajectories.[40] We did not observe a dependence of fluctuation correlation time on the excitation rate, indicating that the fluctuations were spontaneous rather than laser-driven.

We observed autocorrelation rate constants that differed by a factor of 2 over the pH range from 7.2 to 6.0 (Figure 3 and inset): at pH 7.2, the average decay rate constant was $160 \pm 15\ s^{-1}$, and at pH 6.0, the rate constant was $80 \pm 10\ s^{-1}$. This 2-fold decrease in decay rate constant is consistent with the enzymatic activity decrease measured by ensemble-averaged assays at pH 7.2 and 6.0.[35] It has been known that lowering the pH alters the surface charge density of the protein by protonation of the surface carboxylic groups and histidine residues (when substrate is present) and, therefore, perturbs the protein conformation and ultimately the overall enzymatic hydrolysis reaction rate. We found no substrate concentration-dependent fluctuation rates from the single-molecule trajectories at different concentrations of *E. coli* B cells from 0.25 to 2.5 mg/mL. The polysaccharides in the cell wall provide a saturated concentration of the $\beta 1-4$-glycoside bonds for an individual T4 lysozyme molecule. Considering these control experiments of static FRET with and without substrate (Figure 1B), laser excitation intensity dependence, pH dependence (Figure 3), and substrate concentration dependence, we conclude that the anticorrelated fluorescence fluctuations are caused by the protein conformational motions associated with the enzymatic reaction.

Static Inhomogeneity of the Overall Enzymatic Reaction Dynamics of T4 Lysozyme. A 5-fold inhomogeneity in the distribution of autocorrelation function decay rate constants, calculated from 59 single-molecule trajectories, is evident in Figure 3. Similar static disorder in other enzymatic reaction systems has been reported and postulated to originate from different conformers,[2] protein post-translational modifications,[1,3] and proteolytic damage.[6] In this case, we attribute the static inhomogeneity to the differences in local environments among single T4 lysozyme molecules during the enzymatic reaction. Such differences are expected to originate both from topographical inhomogeneity of the *E. coli* B cell walls and from the orientation inhomogeneity of the proteins that are tethered to the hydrocarbon-modified glass surface. We have observed that the tethered proteins are fully mobile and that there is no other perturbation on the activity other than the spatial confinement due to the tethering to the surface.[39]

Autocorrelation functions measured for a large number of single molecules revealed two other decay components, a faster and a slower decay component, compared to the predominant rate component from the single-molecule conformational motion which all single molecules have shown. Ten percent of single molecules showed the slow component and 30% showed the fast component besides the regular component. This observation was made both with and without substrate, indicating that these fluctuations are not related to enzymatic reaction turnovers. These two additional components are independent of laser excitation intensity, suggesting that they correspond to spontaneous conformational changes. Since these two rate components can be distinguished from the rate component of the enzymatic reaction, they must be associated with different quasi-independent nuclear coordinates[40] rather than the enzymatic reaction coordinates.[6] Since dye rotational motions are on a nanosecond time scale, this component at $500\ s^{-1}$ likely originates from intrinsic spontaneous conformational fluctuations[6,39,40,46] of the proteins, which evolve in a widely spread time scale.[47,48] The slow-fluctuation component with rate constant ranging from 1 to $22\ s^{-1}$ in about 10% of single-molecule trajectories is not related to spFRET but is probably due to local-environment changes of the single dye molecules, including a linker-confined protein Brownian motion and the infrequent interactions of the proteins with the hydrocarbon-modified glass surface.[39] The rate-constant distribution of the slow-fluctuation component was distinctively different from the distribution of the conformational change rate constants (Figure 3) associated with enzymatic reactions.

Single-Molecule Conformational Motions under Enzymatic Reaction. To obtain detailed information about the conformational motion associated with the enzymatic turnovers, we further examined the single-molecule fluorescence trajectories. Two types of trajectories were observed. The upper panel in Figure 4 shows an expanded portion of a trajectory (middle panel) recorded from donor fluorescence of a single-pair donor−acceptor-labeled protein with substrate present. By comparison, the lower panel shows a portion of a donor fluorescence trajectory recorded from a donor-only-labeled T4 lysozyme under the same conditions. The large-amplitude, lower-frequency wiggling of the donor fluorescence intensity in the upper panel is largely absent from the trajectory in the lower panel. We interpret each wiggle as a hinge-bending motion involved in either an enzymatic reaction or nonproductive binding and releasing of the substrate. The donor fluorescence increases as the active site opens due to substrate insertion and decreases as the active site closes to form an active enzyme−substrate complex, as discussed previously. We note that the average period (a few milliseconds) of the consecutive wiggles is essentially in agreement with the enzymatic turnover time.[35,49] Hence, it is most likely that the wiggles are associated with

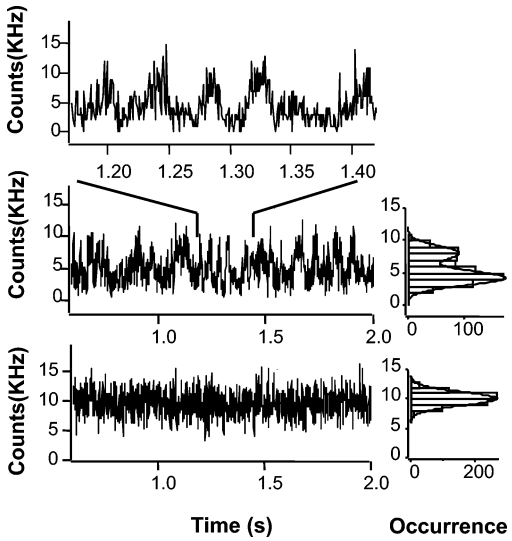

Figure 4. Simultaneous probing of a single T4 lysozyme enzymatic reaction turnover trajectory with correlated hinge-bending conformational motions of the enzyme under hydrolysis of the polysaccharide of a cell wall. The data in the three panels were recorded in 0.65 ms per channel at the same enzymatic reaction condition. The upper panel shows an expanded portion of a trajectory (middle panel) from donor fluorescence of a donor−acceptor-labeled single T4 lysozyme. Intensity wiggles in the trajectory are evident beyond the measurement shot noise. The lower panel shows a portion of a trajectory recorded from a donor-only-labeled enzyme. The fluorescence intensity distributions derived from the two trajectories are shown in the insets of the middle and lower panels. The solid lines are fit using bimodal and Gaussian functions, respectively.

single enzymatic reaction turnovers, leaving only a small fraction of random, nonproductive binding and releasing events. The inset in Figure 4 (middle panel) shows a bimodal fluorescence intensity distribution that reflects the open and closed conformational states of a T4 lysozyme. In contrast, only a Poisson-shaped distribution was deduced from the trajectory of a donor-only-labeled single enzyme molecule. This indicates that only fast fluctuations and uncorrelated noise were recorded, since the donor dye alone is not sensitive to the enzyme open−closed hinge-bending motions (Figure 4, lower panel). The fast fluorescence fluctuation reflects the fluctuation of the local environment around the donor molecule. Similar single Poisson-shaped distributions were always observed from the single donor−acceptor-labeled T4 lysozyme in the absence of substrate.

These simultaneous observations of protein conformational changes and enzymatic reactions in real time allowed us to gain a further molecular-level understanding of the mechanism and dynamics of the complex enzymatic reaction, which is extremely difficult to study in an ensemble-averaged experiment. We propose a mechanism similar to the Michaelis−Menton mechanism (eq 1).

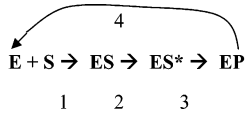

(1)

E, S, and P represent the enzyme, substrate, and product, respectively. ES and ES* represent the enzymatic reaction complex in nonactivated and activated states, respectively. The enzyme and polysaccharide chains engage in a nonspecific interaction through diffusion to form the nonactivated complex state, ES. Then, the active-site cleft binds to a six-glycoside

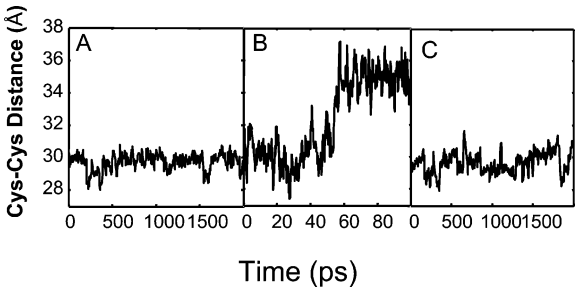

Figure 5. Molecular dynamics simulation of T4 lysozyme hinge-bending motion. Three conformation trajectories of T4 lysozyme in solution at room temperature are presented: free enzyme without substrate (E), active enzyme−polysaccharide complex (ES*), and nonspecific binding of polysaccharide (E + S → ES). (A) Time trajectory of the distance between two −SH groups of Cys 54 and Cys 97 of the free enzyme. (B) Time trajectory of nonactive enzyme−substrate formation dynamics as the polysaccharide moves into the active site of T4 lysozyme. Simulations of the substrate entering the binding site (ES → ES*) were run with the Discover software and included two distance restraints (<1000 (kcal/mol)/Å^2) to pull the ligand into the active site. (C) Time trajectory of the distance between two −SH groups of Cys 54 and Cys 97 of the T4 lysozyme−polysaccharide active complex. In (A) and (C), the enzyme structure (E) was taken from the 1.7 Å X-ray crystallographic structure (PDB entry 3LZM) and included 152 water molecules. The system was placed in a periodic cube of 73.34 Å per side and filled with 11948 SPCE water molecules, including a section of the substrate (ES*). A six-unit oligosaccharide consisting of alternating NAM and NAG was positioned in the active site with the aid of superimposing the lysozyme mutant adducted with substrate cleaved from the cell wall of *E. coli* (PDB entry 148L).

segment of the polysaccharide chain to form specific hydrogen bonds in the activated complex state, ES*.[23] EP represents the enzyme−product complex immediately after completion of the hydrolysis reaction. The subsequent release of product (step 4 in eq 1) and the enzyme searching for the next reactive site in the substrate complete the enzymatic turnover cycle.

MD Simulation of the Binding−Unbinding Conformational Motions under Enzymatic Reaction. We applied MD simulations to further explore the conformations of the intermediate states and the essential conformational change coordinates of the enzymatic reaction in combination with the spFRET data. The calculation of the surface charge densities of the T4 lysozyme and polysaccharide substrate indicates that the substrate, the enzyme active site, and the back surface of the enzyme are negatively charged and the enzyme front surface is positively charged. The binding of T4 lysozyme to the substrate may also involve the amino acids of the substrate. However, as a model, here we only consider a polysaccharide chain involving the enzymatic reaction-associated conformational changes of T4 lysozyme. Hence, it is energetically favorable for the substrate and enzyme to approach each other from the front of the enzyme. Using MD simulation, we sampled the T4 lysozyme conformational states of the enzyme alone (E) (Figure 5A), before its interaction with substrate, the substrate−enzyme complex formation (E + S → ES) (Figure 5B), the enzyme with the polysaccharide substrate in the active site (ES*) (Figure 5C), and the product release (EP → E + P). The equilibrium conformational state of the active substrate−enzyme complex (ES*) (Figure 5C) shows no significant domain displacement compared to the equilibrium conformational state of the free enzyme (E) (Figure 5A). Therefore, the substrate can be in the cavity of the active site and form hydrogen bonds between the substrate and the T4 lysozyme active site without detectable difference from the enzyme's resting conformational state (E). We observed in our MD simulation that there is a narrow gateway to the active site, blocked by an arginine−

glutamic acid salt bridge, which has to be opened before the substrate molecule can diffuse into the active site to form the substrate−enzyme complex (E + S → ES → ES*). When the substrate goes through the gateway to enter the active site, forming the nonactive complex (ES) (Figure 5B), the two domains of the enzyme exhibit a breathing-type hinge-bending motion along the α-helix, causing a 4.5 ± 0.2 Å distance increase between the two cysteines. This motion propagates to a 5.5 ± 0.2 Å increase of the average distance between the donor−acceptor dipoles. This result is consistent with that of the donor and acceptor emission intensity changes measured in the spFRET trajectories, in which more than 2 times the donor emission intensity can be observed. Our MD simulation results suggest that neither the hydrolysis nor product release requires a significant conformational domain displacement. The T4 lysozyme catalyzes the hydrolysis of a *β*-glycosidic bond between an *N*-acetylmuramate (NAM)−*N*-acetylglucosamine (NAG) unit of a polysaccharide substrate. The products (two pieces of NAM-end and NAG-end polysaccharide chains) diffuse out from both sides of the active site without involving hinge-bending conformational motion in an entropy-favored spontaneous process.

The distance change upon substrate binding has difference values reported in the literature based on difference experiments.[20−25,29] Static structure measurements using EPR showed the unligated (substrate-free) form is more open than the substrate-bound form, while X-ray data suggested the active cleft has to further open in the reaction intermediate step compared to the unligated and ligated forms.[23] However, no dynamic measurements have ever been done to identify the scale of the dynamic hinge-bending motion under interaction with the substrate, which is extremely difficult to achieve in ensemble-averaged experiments using the currently available structure analysis tools, NMR, X-ray crystallography, and EPR. Interestingly, previous MD simulations[30] have shown the substrate-free conformation in solution may have either a more opened conformation or a closed conformation comparing the X-ray crystallography data. Our MD simulation also indicates that the substrate-free conformation in solution is opened up slightly compared to the structure from X-ray crystallography, and our MD simulation on the polysaccharide substrate-bound protein conformation in solution is the first to be reported. The reason that our MD simulation did not show the more opened substrate-free conformational state might come from limited simulation time and distance restraints in our MD snapshot simulations. The possibility that the substrate-free conformation has a more opened active site may result in slightly different interpretations of the distance increase and decrease at each stage of the enzymatic reaction shown in eq 1 (t_{open} includes steps 1 and 2 from our MD simulation, or t_{open} includes steps 1, 2, and 4 if E is considered an open substrate-free conformational state). However, under all interpretations, one hinge-bending open−closed time is one fluorescence intensity increase and decrease cycle. Furthermore, all interpretations agree that ES* is a "closed" structure, and to let the substrate in, the structure has to be "open", since the active-site entrance held by the Arg 137−Glu 22 salt bridge is not big enough for taking the polysaccharide chain. Therefore, the conformational difference for the substrate-free and substrate-bound proteins will not affect the interpretation of the reaction mechanism and the hinge-bending motion that we probed. Even if there is no further-opened reaction intermediate, the time of substrate−enzyme complex formation (steps 1 and 2) is still included in t_{open}. Current knowledge of the dynamic and static reaction intermediate states is still insufficient and needs to be enhanced by more systematic protein structure studies, including studies on both static and dynamic structures both with and without substrate interactions. Nevertheless, our ensemble-averaged FRET data support the existence of a further-opened reaction intermediate state associated with the formation of substrate-bound enzyme because that lower FRET efficiency was observed with the substrate versus without the substrate (Figure 1B). Here we interpret our single-molecule fluorescence intensity time trajectories on the basis of both our MD simulation (Figure 4) and experimental results.

The single-molecule donor−acceptor fluorescence trajectories recorded the real-time conformational changes under enzymatic reaction turnovers. The donor−acceptor distance and the donor fluorescence intensity increase when the active site opens up to form a nonspecific binding complex (ES) with the substrate, corresponding to the process of E + S → ES. The donor−acceptor distance and the donor fluorescence intensity decrease when the active site closes to form an active complex (ES*), corresponding to the process of ES → ES*. There are no measurable spFRET changes, implying no significant conformational motions, in the process ES* → EP or in the product-releasing process of EP → E + P. Therefore, the donor fluorescence intensity in a single-molecule time trajectory increases in step 1, decreases in step 2, and remains low in steps 3 and 4 (eq 1). The hydrolysis reaction occurs at step 3. Possible nonproductive binding and release of substrate might give a similar trajectory behavior. However, as we discussed above, we suggest that the occurrence of that type of event is statistically insignificant on the basis of the estimation of an ensemble-averaged reaction rate.

Distribution of the Enzymatic Reaction Complex Formation Time. The formation of ES and ES* involves significant domain breathing-type hinge-bending motions along the α-helix and is probed in real time by recording single-molecule spFRET trajectories. To quantitatively analyze the real-time trajectories, we obtained an intensity threshold[44] corresponding to 50% of the ES-state peak height[50] for counting the duration of the open time (between steps 1 and 2), by fitting the fluorescence intensity distributions of each T4 lysozyme examined (Figure 4, middle panel inset). Those very short open events, which last less than three binning times, cannot be reliably differentiated from shot noise and are not counted as open events. Although some short open events are ignored, the statistics of open states longer than three binning times are not affected. The enzymatic hydrolysis reaction and product release occur following ES* formation, which corresponds to the early part of the closed time. The rest of the closed time is due to the enzyme searching for the next reactive site in the substrate. Using the 50% threshold as a long-pass filter,[50] we were able to read out the formation times, t_{open}, of enzymatic intermediate ES and ES* states from the single-molecule enzymatic turnover trajectories. A typical single-molecule trajectory contains about 15−35 turnovers before the irreversible photobleaching of either the donor or acceptor occurs. Counting the duration of the closed time, t_{closed}, corresponding to ES* → EP → E + P and the enzyme searching for the next reactive site in the substrate, we found a wide range (10−250 s^{-1}) of rate constants[51] among the single molecules examined, showing a significant inhomogeneity among the single molecules under the same physiological conditions. t_{closed} is predominately associated with the enzyme searching for the next reactive site in the substrate because the hydrolysis and product-releasing rates are presumably fast.[52] Thus, the static inhomogeneity of the overall reaction rate constants (Figure 3)

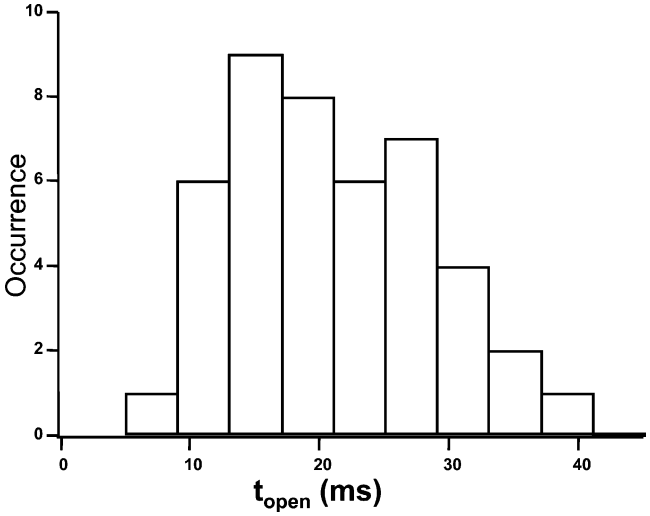

Figure 6. Active complex, ES*, formation time (t_{open}) distribution deduced from a single T4 lysozyme fluorescence trajectory under enzymatic reaction. t_{open} is the duration time of each wiggling of the intensity trajectory above a threshold. The threshold is determined by 50% of the bimodal intensity distribution (see Figure 4, inset). The mean open time, $\langle t_{open}\rangle$, is 19.5 ± 2 ms, and the standard deviation of the open time is 8.3 ± 2 ms.

is most likely due to the time required for the enzyme searching for reactive sites in the substrate. This enzyme searching time is slow and inhomogeneous because the process is sensitive to the inhomogeneous local environment of the single T4 lysozymes and substrate. Since the protein remains in a closed state during these processes, spFRET is not sensitive to this portion of the enzymatic turnover cycle.

Figure 6 shows a Gaussian-shaped distribution of the open time (t_{open}), deduced from a single-molecule trajectory. The first moment of the distribution, $\langle t_{open}\rangle = 19.5 \pm 2$ ms, corresponds to the mean time of the processes of E + S → ES → ES*. The standard deviation of the distribution, $\sqrt{\langle \Delta t_{open}{}^2\rangle} = 8.3 \pm 2$ ms, reflects the distribution bandwidth. We found that the first and second moments of the single-molecule t_{open} distributions are homogeneous, within the error bars, among the individual T4 lysozyme molecules examined under the same enzymatic reaction conditions. Thus, the t_{open} distribution is homogeneous; there is no static disorder in the ES and ES* formation involving hinge-bending motions. The same active-site conformation for a substrate−enzyme complex is induced and attained by protein binding to a glycosidic bond between NAM and NAG in a polysaccharide chain;[21,23] i.e., the enzyme active-site conformations are induced to fit an identical molecular structure of the substrate during each cycle of the enzymatic reaction turnover. The hinge-bending motion allows sufficient structural flexibility for the enzyme to optimize its domain conformation: the donor fluorescence essentially reaches the same intensity in each turnover, reflecting the domain conformation reoccurrence. Therefore, a common structure of the enzyme−substrate complexes controls the subsequent course of the reaction.

The Gaussian-shaped distribution of t_{open} and the ramping changing of the intensity on a millisecond time scale in the single-molecule fluorescence time trajectories suggest that the protein hinge-bending conformational changes involve multiple intermediate conformational states. The dominant nuclear coordinate should be essentially the same for the bending motion that opens and closes the active site and, most likely, is associated with the α-helix hinge of the T4 lysozyme. The results of the MD simulation suggest that the dominant driving force for E + S → ES formation is the positive surface charge of the enzyme from surface amino acid residues (arginine and lysine) interacting with the negatively charged polysaccharide substrate. The driving force for ES → ES* includes formation of six hydrogen bonds in the active site of ES*.

Model Analysis of the Conformational Change Energy Landscape. We model the hinge-bending motion associated with interactions between the enzyme and substrate as a classical particle one-dimensional multiple-step random walk in the presence of a force field,[53] $\{n(t)\}$, where $n(t)$ is the step index. The k_f and k_b are the forward and backward step rate constants, respectively. The driving force would tend to make $k_f > k_b$. The position distribution density function $P_n(t)$ can be calculated[54] by

$$\frac{dP_n(t)}{dt} = k_f P_{n-1}(t) + k_b P_{n+1}(t) - (k_f + k_b)P_n(t) \qquad (2)$$

We then obtain the first moment $\langle n(t)\rangle = (k_f - k_b)t$ and $\langle \Delta n(t)^2\rangle = (k_f + k_b)t$.[55] The $\langle n(t)\rangle$ and standard deviation $\sqrt{\langle \Delta n(t)^2\rangle}$ reflect the drifting and the spreading of the probability $P_n(t)$, respectively. Assuming the random-walk step size of L and a drifting distance of $X_n = nL$, we have $\langle \Delta X_n(t)^2\rangle = L^2(k_f + k_b)t$ and $\langle X_n(t)\rangle = L(k_f - k_b)t$. Considering the one-dimensional random walk and approximate Gaussian shape of $P_n(t)$,[56] we have

$$D = \frac{\langle \Delta X_n(t)^2\rangle}{2t} = \frac{L^2(k_f + k_b)}{2} \qquad (3)$$

and

$$\langle v\rangle = \frac{\langle X_n(t)\rangle}{t} = L(k_f - k_b) \qquad (4)$$

where $\langle v\rangle$ is the mean drifting velocity of the conformational change along the α-helix coordinate. With the approximation of

$$\frac{\sqrt{\langle \Delta X_N(t)^2\rangle}}{\langle X_N(t)\rangle} = \frac{\sqrt{\langle \Delta t_{open}{}^2\rangle}}{\langle t_{open}\rangle} \qquad (5)$$

at long-time limit, where N is the index of the final state, we have

$$D = \frac{(\sqrt{\langle \Delta t_{open}{}^2\rangle}\langle X_N(t)\rangle)^2}{2\langle t_{open}\rangle^3} \qquad (6)$$

where D is the diffusion coefficient. The total drifting distance of the conformational open−close cycle, $\langle X_N(t)\rangle$, is about 9 Å, on the basis of our MD simulation (Figure 5). The mean open time, $\langle t_{open}\rangle$, and the standard deviation of the open-time distribution, $\sqrt{\langle \Delta t_{open}{}^2\rangle}$, are measured to be 19.5 ± 2 ms and 8.3 ± 2 ms, respectively. Therefore, the mean drifting velocity, $\langle v\rangle$, of the conformational change in E + S → ES → ES* is

$$\langle v\rangle = \frac{\langle X_N(t)\rangle}{\langle t_{open}\rangle} = 4.6 \times 10^{-6}\ \text{cm/s}$$

and the diffusion coefficient (eq 6) is, therefore, $D = 3.8 \times 10^{-14}$ cm^2/s.

We further characterized the energy landscape of the hinge-bending conformational change dynamics by estimating the

minimum number of intermediate conformational states involved in the complex formation and by calculating the averaged rates of forming these conformational states. From eqs 3 and 4, we have $D/\langle v\rangle = L[(k_f + k_b)/2(k_f - k_b)]$, and $L = 2D/\langle v\rangle = 1.6$ Å, when $k_b \rightarrow 0$; therefore, the minimum number of conformations is $m = \langle X_N(t)\rangle/L = 5.6$. The average rate for each step is $m/\langle t_{open}\rangle = 280\ s^{-1}$. This result ($m > 2$ at the limit of $k_b \rightarrow 0$) suggests that there are more than two conformational intermediate states in addition to ES and ES*. With the assumption of $k_b \rightarrow 0$, the friction coefficient can be estimated using the Einstein relationship $\xi = kT/D$, giving $\xi = 1.1$ (erg s)/cm^2. The energy consumed by friction in the drifting process is $E_f = \xi\langle v\rangle\langle X_N(t)\rangle = kT\langle v\rangle\langle X_N(t)\rangle/D = 4.5 \times 10^{-20}$ J. From MD simulation of the E state and the ES* state energies, our best estimate of the total energy change between the two states is −18 kcal/mol (-1.25×10^{-19} J per molecule), which constitutes the energy gains from electrostatic, van der Waals, and hydrogen-bond formation terms. Therefore, we estimated that 36% of the total energy change between E and ES* is spent on the friction along the reaction coordinate. Since the total energy change between the E state and the ES* state is about −18 kcal/mol, assuming six intermediate states would result in an average energy difference of 3 kcal/mol for each associated conformational state along the α-helix coordinate during the hinge-bending motion. We postulate that the activation energy associated with the k_f of the forward step is about 0−5 kcal/mol, considering the slow forward rate and the entropy decrease in the complex formation process.[20,57,58] It is reasonable to assume the energy potential surface along the conformational change nuclear coordinate to be parabolic for each intermediate state. Therefore, the averaged force constant of the potential surface for each intermediate state is calculated to be 3.4−20 (kcal/mol)/Å^2.[59]

Combining analysis of experimental single-molecule time trajectories and the computational molecular dynamics trajectories based on a theoretical model allows the reaction mechanism to be described in detail. This approach provides the microscopic conformational change mean drifting velocity, diffusion coefficient, friction coefficient, and E_f. It also provides information about the existence of the multiple intermediate conformational states involving the enzymatic active complex formation and a detailed characterization of the energy landscape of the complex formation process. This information cannot be obtained by an ensemble-averaged experiment, by only a single-molecule experimental, or by a solely computational approach. The combined approach demonstrated here is essential to achieve the potential of both single-molecule spectroscopy and MD simulations for studies of slow enzymatic reactions and protein conformational change dynamics. Nevertheless, single-molecule spectroscopy is itself a powerful approach for measuring the kinetic rates of individual steps in enzymatic reaction turnovers. It allows one to directly obtain reaction rate constants for specific steps in a complex enzymatic reaction, in contrast to ensemble measurements for nonsynchronized reactions such as this hydrolysis reaction.

We have observed a specific conformational fluctuation of the T4 lysozyme. This conformational fluctuation only happens in the presence of a substrate, which is proven to be related to the enzymatic reaction. There is considerable evidence in the single-molecule spectroscopy experiments and MD simulations suggesting that the specific conformation fluctuation corresponds to the single turnover of the enzymatic reaction. However, a limitation of probing conformational changes of the protein is that the product release is not directly probed. A combined approach to probe both parameters is still a great challenge for single-molecule enzymology and is beyond the scope of the present study. Further experiments, for example, using a small-molecule analogue of the polysaccharide substrate,[49] are needed to monitor the product release process and conformational change simultaneously to identify the single enzymatic turnover events.

Conclusion

We have conducted a single-molecule spectroscopy study of the T4 lysozyme conformational dynamics under enzymatic reaction conditions. Combining single-molecule spectroscopy, molecular dynamics simulation, and theoretical modeling, we have begun to obtain detailed mechanistic information about enzymatic conformational dynamics, including the intermediate enzyme−substrate complex structures and the associated energy landscape. The conformation dynamics of hinge-bending motions associated with enzymatic reaction turnovers are probed by single-molecule FRET trajectories. Correlated with MD simulation of enzymatic reaction "snapshots", single-molecule fluorescence fluctuation trajectories can be assigned to the enzymatic reaction steps. We have found that the time required for the enzyme to locate a binding site dominates the inhomogeneity in the overall reaction rate and that the subsequent steps have homogeneous rates among the individual enzymes examined. Our results are also consistent with a mechanism involving multiple intermediate states involved in the formation of the active enzyme−substrate complex. These results are not obtainable for conventional ensemble-averaged experiments. Our results represent a step forward in achieving the potential for single-molecule methods to unravel the nature of a complex enzymatic reaction that is extremely difficult to study by conventional ensemble-averaged experiments alone.

Acknowledgment. We thank Brian Matthews and Walt Baas for providing us with T4 lysozyme proteins, the recipe for preparing the substrate, and helpful discussions, Steve Colson for critical reading and helpful discussions, Greg Schenter for helpful discussions, and Gordon Anderson for help with the instrument development. This work was supported by the Chemical Sciences Division of the Office of Basic Energy Sciences within the Office of Energy Research of the U.S. Department of Energy (DOE).

References and Notes

(1) Polakowski, R.; Craig, D. B.; Skelley, A.; Dovichi, N. J. *J. Am. Chem. Soc.* **2000**, *122*, 4853.
(2) Xue, Q. F.; Yeung, E. S. *Nature* **1995**, *373*, 681.
(3) Craig, D. B.; Arriaga, E. A.; Wong, J. C. Y.; Lu, H.; Dovichi, N. J. *J. Am. Chem. Soc.* **1996**, *118*, 5245.
(4) Ishijima, A.; Kojima, H.; Funatsu, T.; Tokunaga, M.; Higuchi, H.; Tanaka, H.; Yanagida, T. *Cell* **1998**, *92*, 161.
(5) Noji, H.; Yasuda, R.; Yoshida, M.; Kinosita, K. *Nature* **1997**, *386*, 299.
(6) Lu, H. P.; Xun, L. Y.; Xie, X. S. *Science* **1998**, *282*, 1877.
(7) Ha, T. J.; Ting, A. Y.; Liang, J.; Caldwell, W. B.; Deniz, A. A.; Chemla, D. S.; Schultz, P. G.; Weiss, S. *Proc. Natl. Acad. Sci. U.S.A.* **1999**, *96*, 893.
(8) Weiss, S. *Science* **1999**, *283*, 1676.
(9) Edman, L.; Foldes-Papp, Z.; Wennmalm, S.; Rigler, R. *Chem. Phys.* **1999**, *247*, 11.
(10) Edman, L.; Rigler, R. *Proc. Natl. Acad. Sci. U.S.A.* **2000**, *97*, 8266.
(11) Zhuang, X. W.; Bartley, L. E.; Babcock, H. P.; Russell, R.; Ha, T. J.; Herschlag, D.; Chu, S. *Science* **2000**, *288*, 2048.
(12) Yasuda, R.; Noji, H.; Yoshida, M.; Jr, K. K.; Itoh, H. *Nature* **2001**, *410*, 898.
(13) Xie, X. S. *J. Chem. Phys.* **2002**, *117*, 11024.
(14) Yang, H.; Xie, X. S. *J. Chem. Phys.* **2002**, *117*, 10965.
(15) Zwanzig, R. *Acc. Chem. Res.* **1990**, *23*, 148.

(16) Wang, J.; Wolynes, P. *Phys. Rev. Lett.* **1995**, *74*, 4317−4320.
(17) Schenter, G. K.; Lu, H. P.; Xie, X. S. *J. Phys. Chem. A* **1999**, *103*, 10477.
(18) Agmon, N. *J. Phys. Chem. B* **2000**, *104*, 7830.
(19) Lu, H. P.; Iakoucheva, L. M.; Ackerman, E. J. *J. Am. Chem. Soc.* **2001**, *123*, 9184.
(20) Matthews, B. W. *Adv. Protein Chem.* **1995**, *46*, 249.
(21) Zhang, X. J.; Wozniak, J. A.; Matthews, B. W. *J. Mol. Biol.* **1995**, *250*, 527.
(22) Faber, H. R.; Matthews, B. W. *Nature* **1990**, *348*, 263.
(23) Kuroki, R.; Weaver, L. H.; Matthews, B. W. *Science* **1993**, *262*, 2030.
(24) Wagner, G.; Hyberts, S. G.; Havel, T. F. *Annu. Rev. Biophys. Biomol. Struct.* **1992**, *21*, 167.
(25) Goto, N. K.; Skrynnikov, N. R.; Dahlquist, F. W.; Kay, L. E. *J. Mol. Biol.* **2001**, *308*, 745.
(26) Mulder, F. A. A.; Hon, B.; Mittermaier, A.; Dahlquist, F. W.; Kay, L. E. *J. Am. Chem. Soc.* **2002**, *124*, 1443.
(27) Mulder, F. A. A.; Hon, B.; Muhandiram, D. R.; Dahlquist, F. W.; Kay, L. E. *Biochemistry* **2000**, *39*, 12614.
(28) Llinas, M.; Gillespie, B.; Dahlquist, F. W.; Marqusee, S. *Nat. Struct. Biol.* **1999**, *6*, 1072.
(29) Mchaourab, H. S.; Oh, K. J.; Fang, C. J.; Hubbell, W. L. *Biochemistry* **1997**, *36*, 307.
(30) Arnold, G. E.; Ornstein, R. L. *Biopolymers* **1997**, *41*, 533.
(31) Becktel, W. J.; Baase, W. A. *Anal. Biochem.* **1985**, *24*, 150.
(32) Gassner, N. C.; Baase, W. A.; Lindstrom, J. D.; Shoichet, B. K.; Matthews, B. W. *Techniques in Protein Chemistry VII*; Academic Press: New York, 1997; p 851.
(33) Jia, Y.; Talaga, D. S.; Lau, W. L.; Lu, H. S. M.; DeGrado, W. F.; Hochstrasser, R. M. *Chem. Phys.* **1999**, *247*, 69.
(34) Ishii, Y.; Yoshida, T.; Funatsu, T.; Wazawa, T.; Yanagida, T. *Chem. Phys.* **1999**, *247*, 163.
(35) Tsugita, A.; Inouye, M.; Terzaghi, E.; Streisinger, G. *J. Biol. Chem.* **1968**, *243*, 391.
(36) Hayward, S.; Berendsen, H. J. C. *Proteins: Struct., Funct., Genet.* **1998**, *30*, 144.
(37) Zhuang, X.; Ha, T.; Kim, H. D.; Centner, T.; Labeit, S.; Chu, S. *Proc. Natl. Acad. Sci. U.S.A.* **2000**, *97*, 14241.
(38) Penzkofer, A.; Lu, Y. *Chem. Phys.* **1986**, *103*, 399.
(39) Hu, D.; Lu, H. P. *J Phys. Chem. B* **2003**, *107*, 618.
(40) Lu, H. P.; Xie, X. S. *Nature* **1997**, *385*, 143.
(41) High Performance Computational Chemistry Group, NWChem, A Computational Chemistry Package for Parallel Computers, Version 4.0.1, Pacific Northwest National Laboratory, Richland, WA 99352, 2001.
(42) Wang, J.; Cieplak, P.; Kollman, P. A. *J. Comput. Chem.* **2000**, *21*, 1049.
(43) Chandler, D. *Introduction to Modern Statistical Mechanics*; Oxford University Press: Oxford, 1987.
(44) Yip, W.-T.; Hu, D.; Yu, J.; VandenBout, D. A.; Barbara, P. F. *J. Phys. Chem. A* **1998**, *102*, 7564.
(45) Cross, A. J.; Fleming, G. R. *Biophys. J.* **1986**, *50*, 507.
(46) Dickson, R. M.; Cubitt, A. B.; Tsien, R. Y.; Moerner, W. E. *Nature* **1997**, *388*, 355.
(47) McCammon, J. A.; Gelin, B. R.; Karplus, M.; Wolynes, P. G. *Nature* **1976**, *262*, 325.
(48) Frauenfelder, H.; Sligar, S. G.; Wolyne, P. G. *Science* **1991**, *254*, 1598.
(49) Bienkowska, K.; Taylor, A. *Eur. J. Biochem.* **1979**, *96*, 581.
(50) Colquhoun, D.; Sigworth, F. J. In *Single-Channel Recording*, 2nd ed.; Sakmann, B., Ed.; Plenum Press: New York, 1995.
(51) The rates were obtained by fitting the t_{closed} distributions by single-exponential decay assuming a Poisson process. The exponential-shape distribution indicates only one process in the rate control of the chemical reaction during t_{closed}.
(52) Vocadlo, D. J.; Davies, G. J.; Laine, R.; Withers, S. G. *Nature* **2001**, *412*, 835.
(53) McCammon, J. A.; Northrup, S. H. *Nature* **1981**, *293*, 316.
(54) Using the generation function of $\Phi(\lambda,t) = \sum_{n=-\infty}^{\infty} e^{i\lambda n} P_n(t)$ and the eq 2, $\phi(\lambda,t)$ can be obtained. Then, the first moment, $\langle n(t) \rangle$, and the second moment, $\langle n^2(t) \rangle$, of the distribution probability, $P_n(t)$, can be calculated by $\langle n^k(t) \rangle = (1/i^k)(\partial^k \Phi/\partial \lambda^k)|_{\lambda=0}$.
(55) Oppenheim, I.; Shuler, K. E.; Weiss, G. H. *Stochastic Processes in Chemical Physics: The Master Equation*; MIT Press: Cambridge, MA, 1977.
(56) $P_n(t)$ is a Gaussian distribution if $n \rightarrow \infty$. $P_n(t)$ deviates from Gaussian behavior if n is a finite number. However, this deviation is much smaller than the noise in the experimental measurement of $P_n(t)$. Therefore, the experimental $P_n(t)$ can be considered Gaussian in shape even if n is not large.
(57) Mulder, F. A. A.; Mittermaier, A.; Hon, B.; Dahlquist, F. W.; Kay, L. E. *Nat. Struct. Biol.* **2001**, *8*, 932.
(58) Fritsch, K.; Friedrich, J.; Parak, F.; Skinner, J. L. *Proc. Natl. Acad. Sci. U.S.A.* **1996**, *93*, 15141.
(59) The parabolic potential energy surface is presented by the equation $E = E_0 + \omega(Q - Q_0)^2$. So the energies of two states j and $j + 1$ are $E_j = 3 + \omega Q^2$ and $E_{j+1} = \omega(Q - 1.6)^2$. They cross each other at the $E = 3 + E_a$ point. E_a is about 0−5 kcal/mol. We obtained $\omega = 1.7-10$ (kcal/mol)/Å^2 by solving the equations.